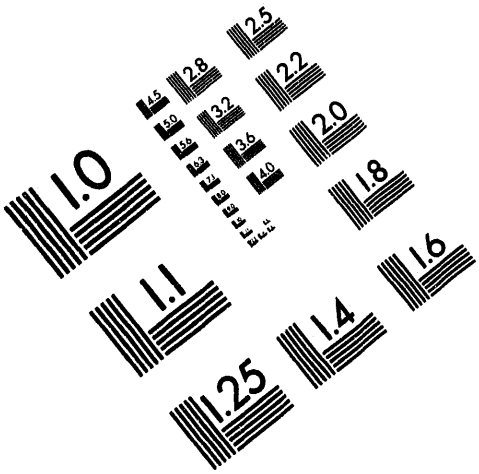

Association for Information and Image Management
1100 Wayne Avenue, Suite 1100
Silver Spring, Maryland 20910
301/587-8202

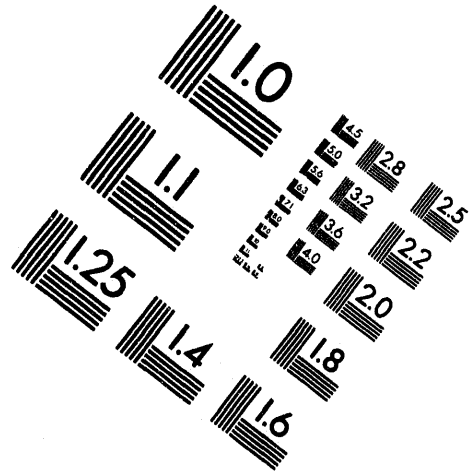

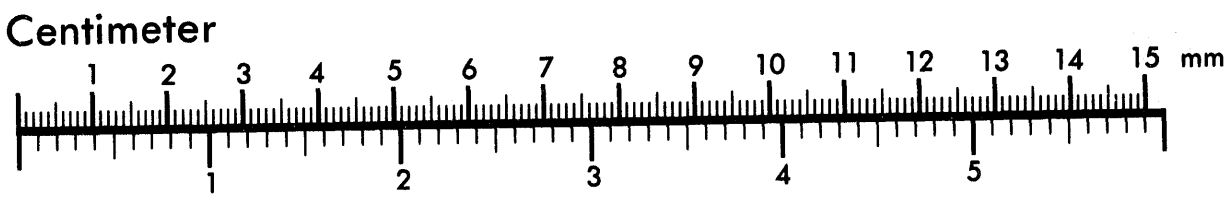

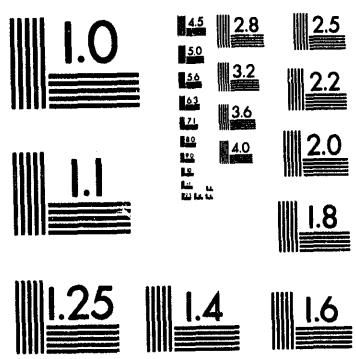

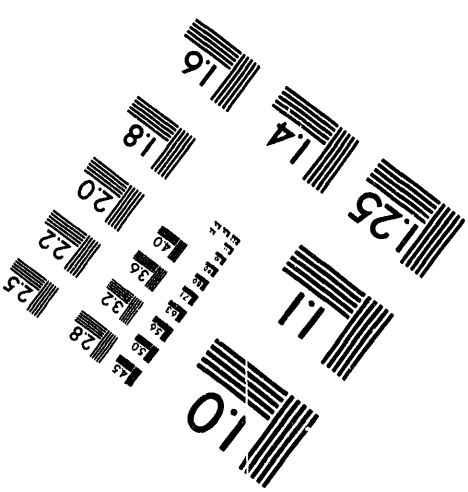

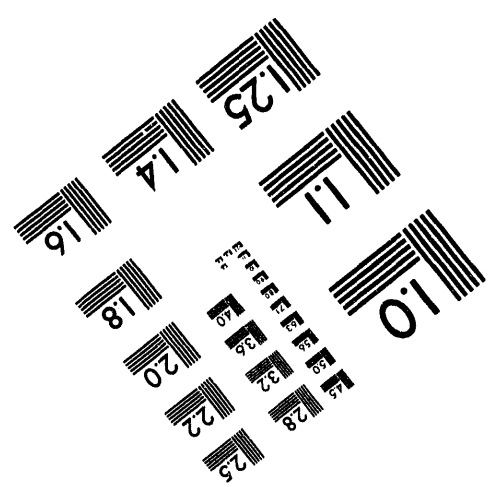

1 of 1

5/6/94

SAND94-0306C

Relation between static and dynamic rock properties in welded and nonwelded tuff

CONF-940642--6

R.H. Price
Sandia National Laboratories, Albuquerque, New Mexico USA

P.J. Boyd, J.S. Noel, R.J. Martin, III
New England Research, Inc., White River Jct., Vermont USA

INTRODUCTION

An integral part of the licensing procedure for the potential nuclear waste repository at Yucca Mountain, Nevada involves accurate prediction of the in situ rheology for design and construction of the facility and emplacement of the canisters containing radioactive waste. The data required as input to successful thermal and mechanical models of the behavior of the repository and surrounding lithologies include bulk density, grain density, porosity, compressional and shear wave velocities, elastic moduli, and compressional and tensile strengths. In this study a suite of experiments was performed on cores recovered from the USW-NRG-6 borehole drilled to support the Exploratory Studies Facility (ESF) at Yucca Mountain. USW-NRG-6 was drilled to a depth of 1100 feet through four thermal/mechanical units of Paintbrush tuff. The thermal/mechanical stratigraphy was defined by Oritz et al. (1985) to group rock horizons of similar properties for the purpose of simplifying modeling efforts. The tuff samples from USW-NRG-6 have a wide range of welding characteristics (usually reflected in sample porosity), and a small range of mineralogy and petrology characteristics. Generally, samples are silicic ashfall tuffs that exhibit large variability in their elastic and strength properties (see Price and Bauer, 1985). The four thermal/mechanical units are designated: TCw, a relatively low porosity welded tuff; PTn, a non-welded very porous tuff sometimes having a high percentage of zeolites and clay; TSw1, a lithophysal rich and vapor-phase altered welded tuff and TSw2 (the potential repository horizon), a welded tuff with relatively few lithophysal cavities and vapor-phase altered zones.

These data constitute a substantial data set to establish correlations between the fracture strength, bulk properties, and elastic properties of the tuff. The emphasis in this study is to collect as much data as possible, in a more or less routine way, on the potential repository horizon and surrounding thermal/mechanical units.

The data collected in the study have both long and short term uses. In the short term, the data are used to characterize the bulk and mechanical properties of the various tuff units for the design of the ESF. On a longer range, these data, combined with specimens tested from other boreholes, will be used to explore the lateral and vertical variability of the tuff to support repository design and performance calculations.

In an effort to characterize the tuffs at Yucca Mountain as thoroughly as possible, compressional and shear wave velocities were routinely measured on all specimens. The velocity data were used in conjunction with the density measurements to compute the dynamic elastic moduli of the rock. These values are compared with the static moduli to infer as much as possible about the pore structure of the rock. A licensed repository will

---

This work was performed under the auspices of the U.S. Department of Energy (DOE), Office of Civilian Radioactive Waste Management, Yucca Mountain Site Characterization Project, under Contract No. DEAC04-76DP900789.

be in existence for thousands of years, and it is important to know as much as possible about the variability in the rocks and their properties for prediction of the properties of the surrounding rock mass. The most remotely measured geophysical parameter is compressional wave velocity. Therefore, it would be useful to establish a scaling law that incorporated fracture strength, Young's modulus, and compressional wave velocity. Fracture strength and Young's modulus are important parameters for modeling long term stability behavior of the rock mass at Yucca Mountain.

EXPERIMENTAL PROCEDURE

Right cylindrical specimens of tuff 50.8 mm in diameter and 101.6 mm in length were prepared from forty-eight cores recovered from borehole USW-NRG-6. A single CT (computerized tomography) scan was performed along the specimen axis. Each specimen was dried at 110°C for a minimum of ten days and the dry bulk density was determined. The specimen was then pressure and vacuum saturated with distilled water. Compressional and shear wave velocities were measured for both dry and water saturated conditions.

Unconfined compression tests to failure were performed at a constant axial strain rate of 10^{-5} s^{-1} at room temperature. The specimen was instrumented with LVDT based transducers to monitor the axial and radial deformation. From these data strains were calculated. Static Young's modulus and Poisson's ratio were computed from the stress and strain data between 10 and 50 % of the fracture strength.

EXPERIMENTAL RESULTS

The results of the experiments are summarized in Figure 1a, b, and c. Following the convention of Price and Bauer (1985), fracture strength, Young's modulus, and dry compressional (P) wave velocity are plotted as a function of porosity. Figure 1a shows a decrease in fracture strength with increasing porosity. The data are distinguished according to the individual thermal/mechanical units. The strength of the tuff ranged from 314 to 1.0 MPa as the porosity increased from 5% to near 58%. The strongest specimens were thermal/mechanical unit TCw, a low porosity welded tuff. In contrast PTn, a non-welded porous tuff, exhibited the lowest strengths. The potential repository horizon, TSw2, exhibited strengths between 56 and 236 MPa for porosities between 9 and 18%.

Figure 1b, shows the change in static Young's modulus as a function of the specimen porosity. The modulus ranges from near 40 GPa to less than 1 GPa. Young's modulus decreases with increasing porosity. Although the trend is distinct, there is significant scatter in the observed modulus at each porosity; in some cases as much as a factor of two.

Figure 1c, shows the dry compressional wave velocity as a function of porosity. The velocity decreases with increasing porosity. The scatter is consistent with that observed for other parameters. Dry P-wave velocities were chosen for detailed consideration for two reasons: shear wave data was not obtainable on all specimens; and compressional and shear wave velocities for saturated specimens were difficult to measure.

DISCUSSION

Price and Bauer (1985) reported that Young's modulus and fracture strength for tuffs in the vicinity of Yucca Mountain are related to functional porosity. Functional porosity is defined as the measured porosity plus the volume fraction of montmorillonite. Strength and modulus decreased with increasing functional porosity. Although there were strong

dependencies of fracture strength and modulus on porosity, significant scatter at a fixed porosity was observed. Frequently, the fracture strength differed by as much as a factor of two or three for a given porosity. A similar effect was noted for static Young's modulus. We have plotted the recently collected data as a function of porosity rather than functional porosity in Figures 1a, b and c, because detailed chemical composition of each specimen has yet to be determined.

The relationship between P-wave velocity and porosity is not unexpected based on the static data and forms a useful link between the static and dynamic properties of the rock. Since the goal of establishing a relationship between the static and dynamic properties is to determine the spacial distribution of static properties throughout the potential repository, the P-wave velocity has been plotted as a function of fracture strength and as a function of static Young's modulus in Figures 2 and 3, respectively. Finally, the relationship between static and dynamic Young's modulus is shown in Figure 4. The ratio of dynamic to static moduli is very instructive in establishing the microstructure of the tuff.

The analysis of the data has concentrated on two aspects. First, the relationship between the static and dynamic moduli, and second, the relation between dynamic properties, such as compressional wave velocity, and fracture strength. Specifically, it is important to understand why the dynamic moduli are consistently greater than the static moduli and the reason for the scatter in fracture strength and moduli at a fixed porosity.

Both the static and dynamic moduli have been measured on a wide variety of rocks (e.g. Simmons and Brace, 1965; Cheng and Johnston, 1981; Jizba, 1991). Generally, for a specific rock type, the dynamic moduli exceed the static moduli. For specimens from USW-NRG-6 the ratio of the dynamic to static moduli ranges from 1.13 to 2.17.

The elastic properties and fracture strength of most brittle rocks have been modeled in terms of the pore size and geometry. Elastic constants, as well as compressional and shear wave velocities have been shown to be related to the micro-crack density, crack length and the shape of the pores (e.g. Walsh, 1965; O'Connell and Budiansky, 1974; Mavko and Nur, 1978). Each of these models showed that with increasing crack length and crack density the bulk modulus, Young's modulus, and compressional wave velocity decrease. While these models establish the dependence of porosity on elastic properties, they do not offer insight into the differences between static and dynamic elastic moduli widely reported and present in the tuffs at Yucca Mountain.

The fracture strength of brittle rocks are strongly controlled by the initial damage. Damage typically consists of micro-cracks and irregularly shaped pores that act as stress concentrators and loci for crack initiation and propagation (e.g. Costin, 1983; Sammis and Ashby, 1986; Holcomb, 1993). Given that, both the elastic and deformational properties are controlled by the distribution and size of cracks and pores, the correlations between static and dynamic rock properties as shown in Figures 2, 3 and 4 are reasonable. In many studies, a single rock type with well defined properties, such as granite or sandstone, has been studied in detail to examine the effect of one variable on the static and dynamic properties and/or strength.

At Yucca Mountain, a wide variety of tuffs are represented. While the chemical composition of the tuffs is relatively uniform, the differences reside in the porosity, the pore geometry and distribution, and the alteration products within the tuff. For example there are lithophysal and vapor-phase altered zones in TSw1 and TSw2. The objective of collecting dynamic properties of the tuff is to ultimately correlate them with the mechanical properties and to use the empirical relationships to assess the lateral variability in each lithologic unit throughout Yucca Mountain. As we have seen, the fracture strength and elastic properties of tuff can be related, at least to a first order, to porosity. However, within a given lithology even specimens with nearly the same porosity exhibit properties that can differ by as much as a factor of two.

The CT scans allow us to examine the shape and distribution of pores in the specimen. In some cases, the pores are relatively large and easily resolved. The data from four specimens representing end members for the ratio of dynamic to static Young's modulus (E) were selected for analysis. Two specimens from TSw1 recovered from 427.0 and

488.0 feet and two specimens from TSw2 recovered from 953.2 and 985.7 feet depth were analyzed. The properties measured on each of these specimens are shown below. Although the differences in porosity for the specimens within each unit are relatively small, there are large differences in the fracture strength, compressional and shear wave velocities, and static and dynamic Young's modulus.

The CT scans for the four specimens are shown in Plates 1 and 2. The lighter the shading the lower the density of the material represented in the scan. In order to quantitatively assess the relative proportion and distribution of pores within each scan image analysis has been performed. We are looking for the volume fraction of the pores, the largest contiguous pore, and the mean size of the pores. For the TSw1 specimens (Plate 1), the volume fraction of low density material in 427.0 is approximately fourteen times greater than that for 488.0. Furthermore, zones of low density material are larger by a factor of nearly twenty. The difference in porosity between the two specimens is small, but the differences in the distribution and characteristic length of the pores is large. From a qualitative point of view, if the strength and the dynamic properties of the rock are related to the size and shape of the pores specimen 427.0 should be weaker and exhibit lower moduli and velocities than 488.0.

Two specimens from TSw2, are shown in Plate 2. The distribution of low density zones in these two specimens is not as pronounced as those for TSw1. Specimen 953.2 is characterized by large light colored zones representing vapor-phase altered regions. A relatively large lithophysae is apparent in the upper right quadrant of the specimen. In contrast, the vapor-phase altered regions for 985.7 are much smaller and not as pronounced. The large percentage of weak, low density, vapor-phase altered zones in 953.2 contribute to the low strength, velocity, and static modulus.

Bulk and Mechanical Properties Data for Four Specimens from USW-NRG-6

Unit	TSw1	TSw1	TSw2	TSw2
Depth, ft	427.0	488.0	953.2	985.7
Porosity, %	14.1	10.5	17.6	9.9
Grain Density, gcm^{-3}	2.527	2.504	2.548	2.554
P-Velocity, km s^{-1}	3.463	4.299	4.054	4.499
S-Velocity, km s^{-1}	2.228	2.684	2.408	2.812
Strength, MPa	43.4	149.4	31.6	177.3
Static E, GPa	14.2	33.3	16.9	37.6
Dynamic/Static E, GPa	1.74	1.13	1.77	1.14

The variations in pore structure for the specimens shown from TSw1 and TSw2 support the differences in P-wave velocity, Young's modulus, and fracture strength. As lithophysae and vapor-phase altered zones increase in size and abundance, the elastic moduli and fracture strength decrease. This is one of the first of several wells that have been and will be drilled at Yucca Mountain in support of the ESF design. As the data set increases and image analysis is performed on CT scans from each specimen, a relation between statistical properties of the pore structure and the mechanical properties of tuff will be developed. However, it is clear that it will not be possible to give an unequivocal explanation for the differences between the static and dynamic Young's modulus. In a previous study (Martin et. al, 1992) Young's modulus was measured as a function of strain amplitude and frequency for a specimen of TSw2. In the dry state there was no dispersion in Young's modulus at frequencies between 10^{-2} to 10^{6} Hz. Furthermore, at strains between 10^{-6} to 10^{-5} Young's modulus was constant for a fixed loading frequency of 10^{-2} Hz. These results suggest that the pores in welded tuff are elliptical to spherical and do not result in a significant difference between the static and dynamic moduli. With saturation however, the dynamic moduli increases and the static moduli should decrease. In this case, we are comparing dry dynamic moduli with saturated static moduli. If all the pores were elliptical and spherical one would anticipate the static and the dynamic moduli

would be very near equal. The fact that the differences are large in some cases indicates that there are a number of effects influencing the behavior of the rock; most likely these include strain amplitude, chemical weakening of the bonds along grain boundaries, particularly in specimens of PTn, and the effect of strain amplitude on the closure of cracks and pores in some units.

CONCLUSION

A large data set has been collected on specimens recovered from borehole USW-NRG-6. Analysis of the results of these experiments showed that there is a correlation between fracture strength, Young's modulus, compressional wave velocity and porosity. Additional scaling laws relating; static Young's modulus and compressional wave velocity; and fracture strength and compressional wave velocity are promising. Since there are no other distinct differences in material properties, the scatter that is present at each fixed porosity suggests that the differences in the observed property can be related to the pore structure of the specimen. Image analysis of CT scans performed on each test specimen are currently underway to seek additional empirical relations to aid in refining the correlations between static and dynamic properties of tuff. Once these studies are complete it may then be possible to examine in more detail possible mechanisms to explain the differences between static and dynamic moduli and refine the interpretation of the dependence of fracture strength and static Young's modulus on acoustical measurements, such as compressional wave velocity.

REFERENCES

Cheng, C.H. and D.H. Johnston 1981. Dynamic and static moduli. Geophys. Res. Let.. 8:39-42.

Costin,L.S. 1983. A microcrack model for the deformation and failure of brittle rock. J. Geophys. 88:9485-9492.

Holcomb, D., 1993. General theory of the Kaiser effect. 34 U.S. Symposium on Rock Mechanics, University of Wisconsin-Madison 2:423-430.

Jizba, D.L. 1991. Mechanical and acoustical properties of sandstones and shale. Thesis submitted to the Department of Geophysics, Stanford University.

Martin R.J., III et. al, 1992. Modulus dispersion and attenuation in tuff and granite. Proceedings of the 33rd U.S. Symposium on Rock Mechanics. 899-908.

Mavko G.M and A. Nur, 1978. The effect of Nonelliptical cracks on the compressibility of rocks. J. Geophys. Res. 83:4459-4468.

O'Connell, R. and B. Budiansky, 1974. Seismic velocities in dry and saturated cracked solids. J. Geophys. Res. 79:5412-5426.

Oritz, T.S., R.L. Williams, F.B. Nimick, B.C. Whittet, and D.L. South 1985. A three dimensional model of freference thermal/mechanical and hydrologic stratigraphy at Yucca Mountain, Southern Nevada. SAND84-1076, Sandia National Laboratories Albuquerque, NM.

Price, R.H. and S.J. Bauer 1985. Analysis of elastic and strength properties of Yucca Mountain tuff, Nevada. Research and Engineering Applications in Rock Masses. Proceedings of 26th U.S. Symposium on Rock Mechanics, Eilleen Ashworth (ed) 1:89-96.

Sammis, C.G. and M.F. Ashby 1986. The failure of brittle porous solids under compressive stress states. Acta metall. 34:511-526.

Simmons, G and W.F. Brace 1965. Comparison of static and dynamic measurements of compressibility of rocks. J. Geophys. Res. 70:5649-5656.

Walsh, J., 1965. The effect of cracks on the compressibility of rock. J. Geophys. Res. 70:381-389.

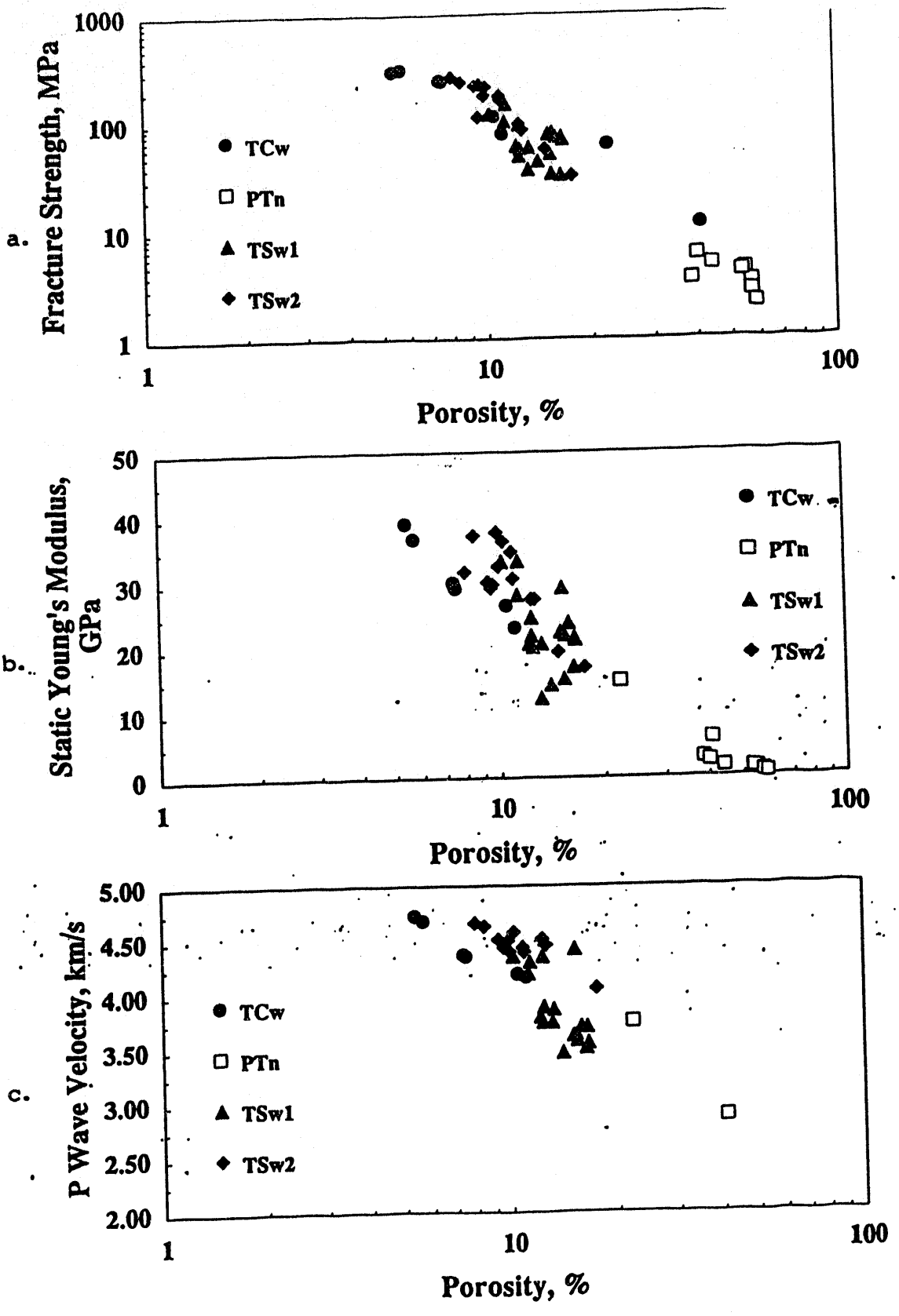

Figure 1: Fracture strength (a), static Young's modulus (b), and P-wave velocity (c) are plotted as a function of porosity for specimens for USW-NRG-6 tested in uniaxial compression.

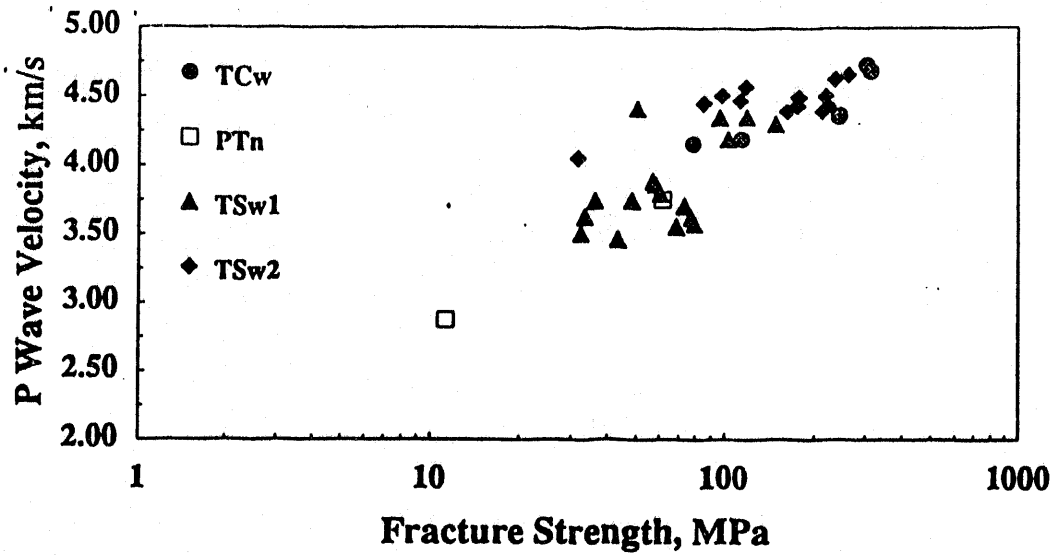

Figure 2: P-Wave velocity is plotted as a function of fracture strength for specimens of USW-NRG-6 tested in uniaxial compression.

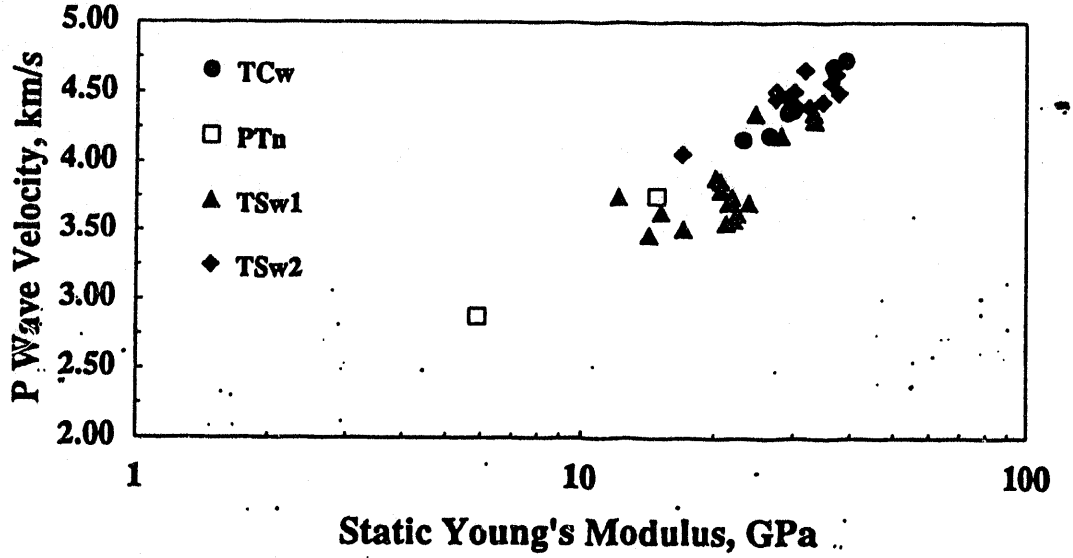

Figure 3: P-Wave velocity is plotted as a function of static Young's modulus for specimens of USW-NRG-6 tested in uniaxial compression.

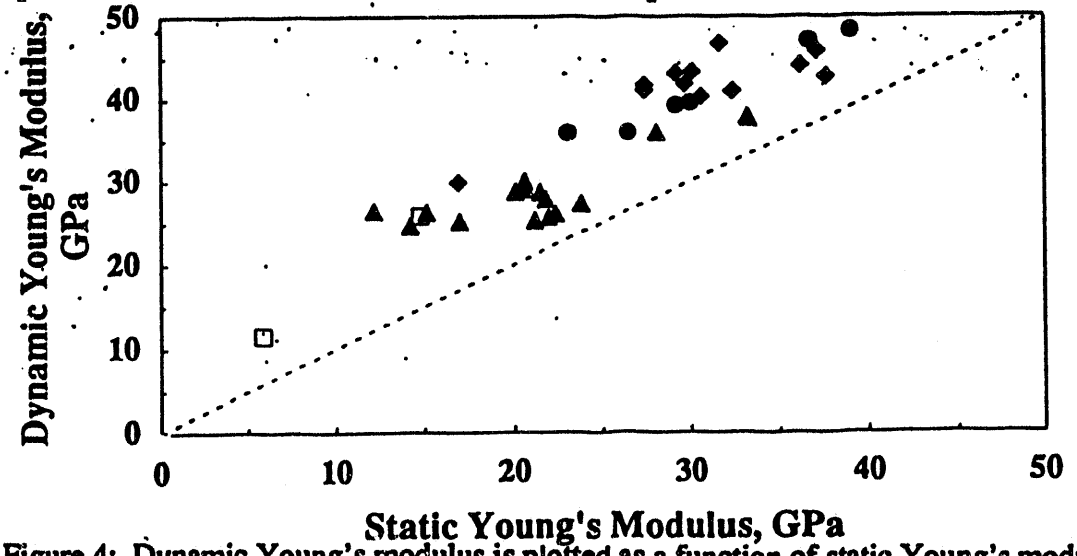

Figure 4: Dynamic Young's modulus is plotted as a function of static Young's modulus for specimens of USW-NRG-6 tested in uniaxial compression.

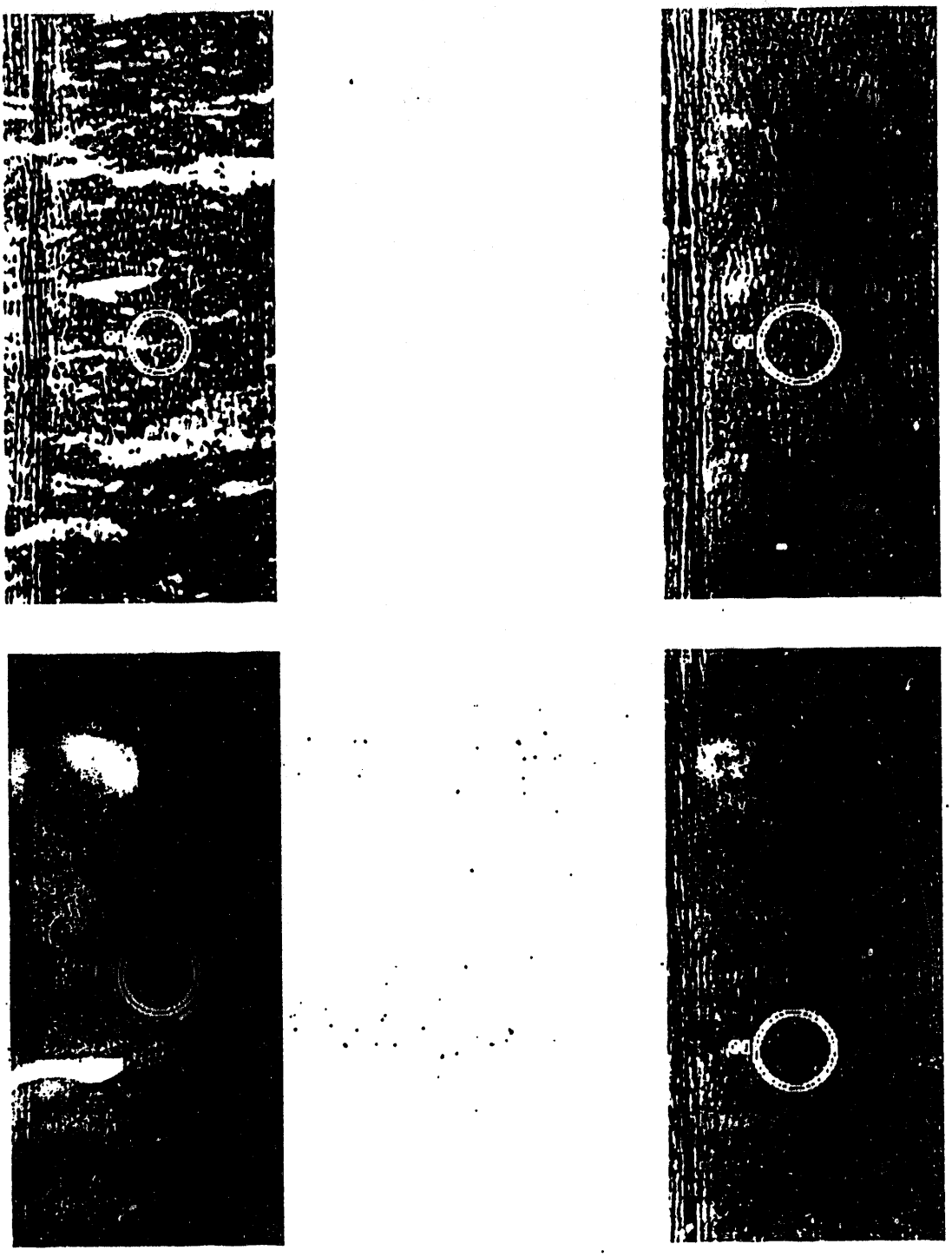

Plates 1 and 2: CT scans for TSw1 specimens 427.0 and 488.0 (top left and right) and TSw2 specimens 953.2 and 985.7

DATE
FILMED
7/29/94
END